Graph Spectra of Carbon Nanotube Networks

Stephen F. Bush, *Senior Member, IEEE, GE Global Research Center*

Sanjay Goel, *Member IEEE, University at Albany, SUNY*

Abstract— Sensor coverage will benefit from finding better ways to communicate among smaller sensors. Also, as development in nanotechnology progresses, the need for low-cost, robust, reliable communication among nano-machines will become apparent. Communication and signaling within newly engineered inorganic and biological nano-systems will allow for extremely dense and efficient distributed operation. This paper examines these potential benefits from the perspective of using individual nanotubes within random carbon nanotube networks (CNT) to carry information. One may imagine small CNT networks with functionalized nanotubes sensing multiple elements inserted into a cell in vivo. The information from each nanotube sensor can be fused within the network. This is clearly distinct from traditional, potentially less efficient, approaches of using CNT networks to construct transistors. The CNT network and routing of information is an integral part of the physical layer. Single-walled carbon nanotubes (SWNT) are modeled as linear tubes positioned in two dimensions via central coordinates with a specified angle. A network graph is extracted from the layout of the tubes and the ability to route information at the level of individual nanotubes is considered. The impact of random tube characteristics, such as location and angle, upon the corresponding network graph and its impacts are examined.

Index carbon nanotubes, communication networks, and sensor networks.

I. INTRODUCTION

Due to their small size nanotubes can reach deep into their environment without affecting their natural behavior. For example, a single CNT is small enough to penetrate a cell without triggering the cell's defensive responses. Individual nanotubes can be used to construct a network of sensing elements. The depth and coverage provided by such a network of sensing elements would be greater than today's sensor networks. Unfortunately, networking such a collection of sensors using current techniques, including wireless techniques, negates the advantages of the small CNT size. The solution proposed in this paper is to use the random CNTs themselves as the communications media, thus bringing the scale of the network down to the scale of the sensing elements.

Current technology is focused on utilizing an entire CNT network as semiconducting material to construct a single transistor or Field Effect Transistor (FET). Many such transistors are required to build legacy network equipment. The result is that nano-scale networks are embedded within each device that might be otherwise more effectively and directly utilized for communication. Consider re-thinking the communication architecture such that the CNT network itself is the communication media and individual nanotubes are the links. Much research has gone into understanding how to align tubes. Unfortunately, cost and separation of impurities (metallic tubes) is still an unsolved problem. In the approach proposed in this paper, lower-cost, randomly oriented tubes are directly utilized as a communication media. Fig. 1 illustrates a sample communication network where users at a molecular level simultaneously share random CNT network bandwidth. The black lines depict the nanotubes and the dark red lines show input/output channels (or probes) into the network media. Each user has a distinguishable impact on the receiver via network interaction as shown by the range of resistances from each user as shown in the figure.

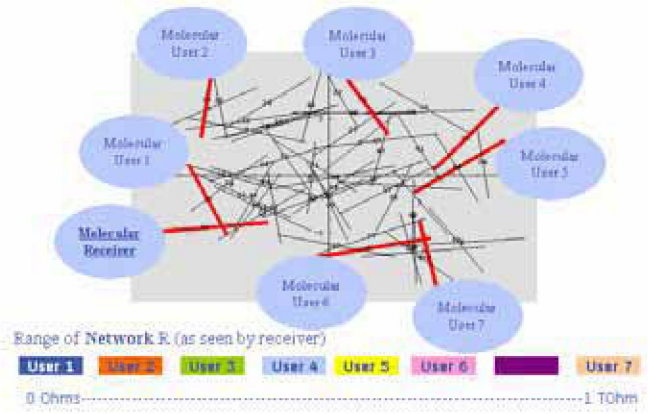

Fig. 1 Routing through an embedded random carbon nanotube network.

To analyze such graphs a spectral analysis is used. Spectral analysis reveals the topological properties of a graph such as

Manuscript received January 30, 2006; intended for submission to Nano-Net 2006.
Stephen F. Bush: GE Global Research Center, Niskayuna, NY, 12309, USA phone: 518-387-6827; fax: 518-387-4042; e-mail: bushsf@research.ge.com.
Sanjay Goel: University at Albany, 1400 Washington Avenue, Albany, NY 12222, Phone: (518) 442 4925; Fax: (518) 442 2568, e-mail: goel@albany.edu.

its patterns of connectivity and typically involves computing the eigenvalues and eigenvectors of the Laplacian matrix of a graph. The Laplacian matrix of a graph is an undirected, un-weighted graph without graph loops or multiple edges from one node to another. The eigenvalues are related to the topology of the graph and represent specific features. For instance, the second smallest eigenvalues represents the measure of compactness of a graph. A large value implies a compact graph where as a small value represents an elongated graph. Such an analysis is often used for relative comparisons of graphs; however, only graphs with the same number of vertices can be meaningfully compared. Spectral analysis has been used in a wide variety of applications, including, semantic analysis of documents to cluster documents into areas of interest, comparing structural, functional and evolutional similarity in RNA molecules, connectivity on the Internet, etc. Though very elegant there are some limitations to this technique. For instance, Mihail and Papadimitriou [8] argue that for randomly generated graphs that satisfy a power law distribution, spectral analysis of the adjacency matrix will simply produce the neighborhoods of the high degree nodes as its eigenvectors and miss any embedded structure. For graphs that do not have skewed degree distributions, however spectral analysis is an efficient tool that reveals inherent embedded structures. Even for graphs with skewed degree distributions transformations can be applied to enable spectral analysis in recovering the latent structure with a high probability [5]. A graph spectral technique precisely solves the problem of determining resistance through the random tube layouts and is applied to the analysis of the CNT graphs to reveal their inherent structural properties, discussed later in this paper.

In this paper, the impact of scale on a traditional communication network is considered as the network is scaled down to the size of a carbon nanotube network. An obvious consideration from a network perspective is the change in capacity, specifically in bandwidth. Simple harmonic oscillation, which provides bandwidth, increases with reduction in scale; thus potential bandwidth increases dramatically [9]. The increase is 1/L where L is a linear scale dimension. The capacity, C_{ij}, of a link from a transmitter at j to a receiver at i is given by Shannon's famous formula (1). Considering all possible multi-level and multi-phase encoding techniques, the theorem states that the theoretical maximum rate of clean (or arbitrarily low bit error rate) data with a given average signal power that can be sent through an analog communication channel subject to additive, white, Gaussian-distribution noise interference is:

$$C_{ij} = BW \ln(1 + (S/N)_{ij}) \quad (1)$$

The term BW is the bandwidth of the communication and $(S/N)_{ij}$ is the signal-to-noise ratio (SNR) of the link. SNR measures the ratio between noise and an arbitrary signal on the channel, not necessarily the most powerful signal possible. In Fig. 2, the channel capacity, assuming that the noise is minimal (SNR=1/2), rises as the scale is reduced towards zero using (1).

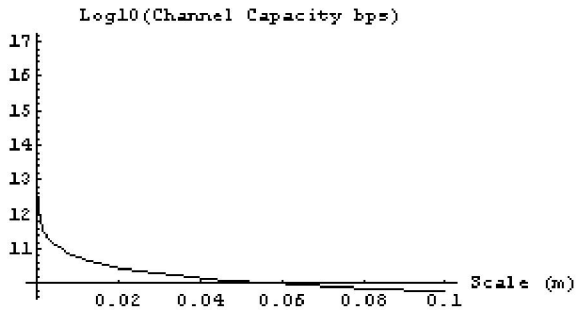

Fig. 2 The approximate capacity increase with reduced scale is shown. As the scale becomes smaller, the potential capacity grows significantly.

In addition to the increased bandwidth potential, the nanotube density allows for an increase in the number of bits per square meter. Consider a wireless network of today. A typical bit-meters/second capacity is limited in a traditional wireless network as described in [6]. The maximum wireless capacity approximation in a wireless broadcast media can be used to determine the collective capacity. Assume a perfect distribution mechanism in which all links are used as efficiently as possible to disseminate route update information [1]. Assume a network of n nodes is spread over an area A and each possible connection has capacity W. Also, assume Δ is a guard distance to ensure channel transmissions do not overlap. The maximum wireless capacity in bit-meters per second is shown in (2).

$$C_{\max} = \sqrt{\frac{8}{\pi}} \frac{W}{\Delta} \sqrt{n} \quad (2)$$

Generalizing to a uniformly random distribution of n sensors over a circular area A, the density is n/A, and the expected nearest-neighbour distance is $\sqrt{A}/n$. The total distance that data must travel is shown in (3).

$$E[d] = \sum_{k=1}^{n} \frac{\sqrt{A}}{n} \quad (3)$$

Now consider a carbon nanotube network. A point source could radiate information omni-directionally via a tube structure limited by the degree of compactness of the tube network. If tubes could be well aligned, then the notion of a guard distance would be unnecessary. A macroscopic source is assumed to generate data omni-directionally. A carbon nanotube is on the order of 1.4 nm in diameter. If tubes radiate compactly from a circular source, the capacity is shown in Fig. 3. Essentially, the limit is reached as an extremely large number of tubes are joined to the source without overlapping. Unfortunately, current technology cannot align tubes with this degree of accuracy.

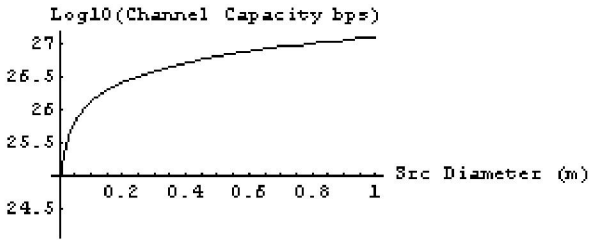

Fig. 3 The capacity of a carbon nanotube network is shown as a function of the area available for nanotube connectivity. This is significantly higher capacity over much smaller distances than could be achieved with a wireless network.

A Mathematica [10] framework for evaluating random CNT networks has been developed and is being used to verify design characteristics of carbon nanotubes. The framework relates tube placement characteristics comprised of tube center location t_{xy}, tube angle θ, and tube density d_t. The intersections of tubes form vertices V and tubes form edges E of a graph $G(V,E)$. In the specific instance of FET mobility, the graph structure impacts the mobility μ of the FET. Thus, a goal has been to find the relationship among tubes, the CNT network, and mobility as shown in (5)[2]. Let $f(t_{xy},\theta,d_t)$ be a function of physical tube characteristics. Mobility is approximated in (4).

$$\mu = \frac{L_{sd}(I_{on}-I_{off})}{w}\frac{t_{ox}}{20\varepsilon V_{sd}} \tag{4}$$

I_{on} and I_{off} are FET gate 'on' and 'off' currents that are determined by the resistance of a CNT network; w and L_{sd} are the gate width and length respectively.

$$f(t_{xy},\theta,d_t) \longrightarrow G(V,E) \longrightarrow \mu(\Delta R_{sd}) \tag{5}$$

A key component of the tube layout is the overall directionality of the tubes, that is, the angle of each tube relative to all other tubes. Isotropy is a measure a global measure of this directionality. Isotropy quantifies the directionality of the tubes and is defined in (6).

$$\frac{\sum l\cos a}{\sum l\sin a} \tag{6}$$

l is the tube length and a is the tube angle. Tubes that are nearly aligned have a high isotropy and tubes that are randomly oriented have a low isotropy. Fig. 4 shows the isotropy of a set of CNT networks with constrained tube angles. The tube density is 1.2 per micron and lengths are constant at 3 microns. The angles range from being constrained between –1 through +1 degrees to –90 through +90 degrees.

[2] A Mathematica package has been developed that constructs a CNT network from a tube layout and has supported the analytical development of CNT network properties.

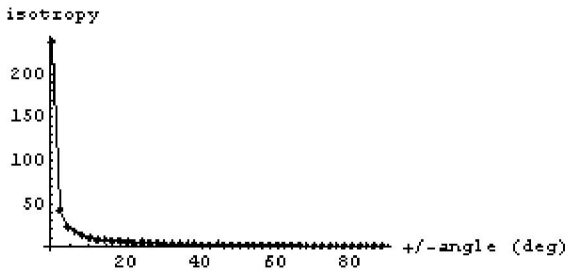

Fig. 4 Isotropy decreases as tube angles assume wider ranges.

The angle of each tube can be considered as encoding information. Entropy, from an information theoretic viewpoint, measures the amount of information. Angle entropy is defined in this paper as $-\sum \Pr(a)\log_2(\Pr(a))$ where a is the tube angle and Pr is the probability of a tube of angle a given the network under analysis. The angle entropy of the network analyzed in Fig. 4 is shown in Fig. 5. Clearly, the more random the angle, the more angular entropy exists and thus there should be a relationship between isotropy, angular entropy, the type of networks that are formed, and ultimately, their performance and resilience to metallic tubes.

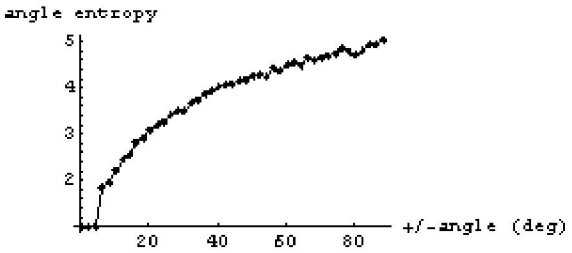

Fig. 5 Angle entropy increases as the range of tube angles increases.

Clearly, there is a relationship between isotropy and angle entropy as shown in Fig. 6 for the same networks analyzed in the previous figure. High angle entropy implies that the directionality and thus the isotropy are low. Information can be stored in tube angles; reading the information from the change in resistance of tube angles is discussed in [3].

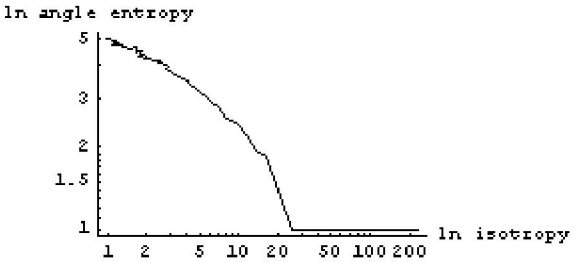

Fig. 6 Natural Logarithm of angle entropy decreases as natural logarithm of isotropy increases.

As isotropy increases and entropy decreases, the density of tube intersections increases as shown in Fig. 7. Greater angular variation enables the tubes to intersect nearer to one another. The inter-tube contact resistance has a greater impact as intersection density increases. There is also an impact on

the probability of percolation, which is considered in detail in a paper being written by the same authors.

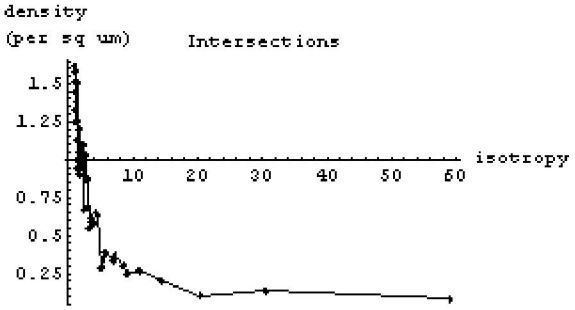

Fig. 7 The density of tube intersections (nodes) varies inversely with isotropy.

II. Characteristics of CNT Networks

For any given orientation of nanotubes, the corresponding network $G(V,E)$ is extracted and resistances are assigned based upon the probability that a tube is either a pure carbon nanotube of 10^6 ohms when the gate is 'on' (10 volts) and 10^{12} ohms when the gate is 'off'. Impure (solid nanotubes) remain at 10^6 ohms regardless of gate voltage and the probability of a solid tube is 0.33.

The network formed by the overlapping nanotubes is extracted by determining the location of junctions. The gate area is overlaid on this network and virtual vertices are added as source and drain; the virtual vertices are assigned edges with no resistance to each nanotube that is adjacent to the source or drain edge of the layout respectively. The equivalent resistance of the network of resistors across the virtual source and drain is determined by (7) where l_i is the ith Eigenvalue of the graph Laplacian and $\varphi_{i\alpha}$ is the α component of the ith eigenvector of the graph Laplacian.

$$R_{sd} = \sum_{1}^{N} \frac{1}{l_i} \left| \varphi_{is} - \varphi_{id} \right|^2 \tag{7}$$

The graphs for large numbers of tube layouts with different distributions of locations, angles, and lengths have been generated. An example is shown in Fig. 8.

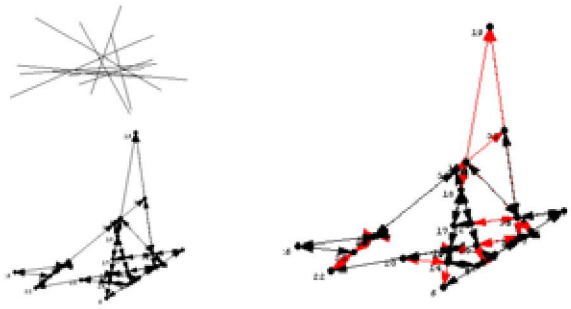

Fig. 8 Example of random CNT network generation: 10 tubes, angles uniformly distributed from 0 through π radians, tube centers are distributed in an area of 5 by 5 microns and tube lengths are randomly distributed from 5 to 20 microns, and the probability of a metallic edge is 0.33. The graph on the right highlights the metallic tubes (red).

Virtual source and drain locations are specified. This results in the addition of virtual nodes representing the source and drain as shown in Fig. 9.

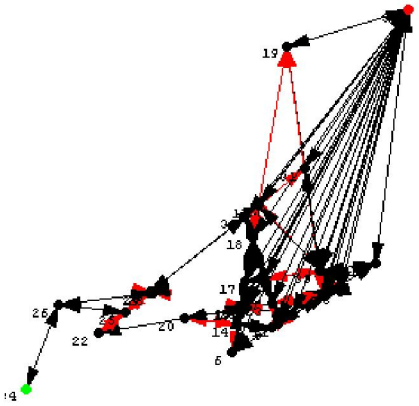

Fig. 9 Virtual source and drain nodes added to the graph from Fig. 8.

Consider the relation in (5), namely, $f(t_{xy}, \theta, d_t) \longrightarrow G(V,E)$. Note that tube center locations t_{xy} and tube angles θ, are random variables. Tube density d_t is the number of tubes per unit area and is not considered a random variable in this analysis. Intuitively, one would expect the anisotropy (8), to have an impact on vertex density d_v.

$$\frac{\sum_{i=1}^{N} \left| \cos\theta_i \right|}{\sum_{i=1}^{N} \left| \sin\theta_i \right|} \tag{8}$$

In (8), the x component of each tube is $L_i \cos\theta_i$ and the y component of each tube is $L_i \sin\theta_i$ where L_i is the length of the *i*th tube. If tube lengths are infinite, the number of vertices in $G(V,E)$ is defined as in (9) where n_t is the number *n* of intersections among tubes *t*. The intuition is that each new tube will overlap with n-1 existing tubes assuming no tubes are exactly parallel, yielding additional n-1 nodes. Fig. 10 shows the number of the extracted graph nodes versus tubes. Tube angles are uniformly distributed from $-\pi/4$ to $\pi/4$ radians and tubes lengths vary uniformly from 3 to 10 microns in a 5 by 5 micron area. The simulation has a lower number of nodes because it assumes infinite tube lengths. The simulated nodes were finite; as the tube lengths increase, it is expected that the actual number of nodes would approach the analytical result.

$$|V| = n_t = \left(\sum_{i=1}^{t-1} t\right) \approx \frac{t^2}{2}, n_1 = 0, n_2 = 1 \qquad (9)$$

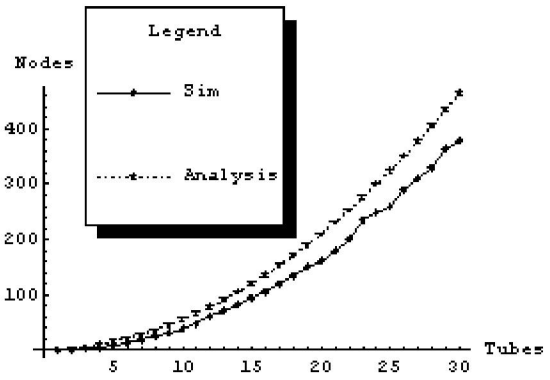

Fig. 10 Simulated versus analytical results for tube angles uniformly distributed from 0 to $\pi/2$ radians. Analytical results assume overlaps from infinite tube lengths, thus the analytical results are an upper bound on the actual number of nodes.

Determining the number and density of vertices when tube lengths are finite becomes more complex. Equation (9) needs to be modified such that each term includes the probability of overlap between tube pairs as shown in (10), (11), and (12) where then probability of overlap is defined in terms of the probability of overlap in both the x and y components of tube pairs. o_t is the number of overlaps among *t* tubes.

$$P_{ij}(o_2) = P_{ij}(o_x)P_{ij}(o_y) \qquad (10)$$

$$P_{ij}(o_y \mid y, L, \theta) = P_{ij}\left(\left|y_i - y_j\right| < \left(L_i \sin\theta_i + L_j \sin\theta_j\right)\right) \qquad (11)$$

$$P_{ij}(o_x \mid x, L, \theta) = P_{ij}\left(\left|x_i - x_j\right| < \left(L_i \cos\theta_i + L_j \cos\theta_j\right)\right) \qquad (12)$$

Combining equations (10), (11), and (12) with (9) yields (13). The analysis from (13) is plotted versus actual in Fig. 11.

$$|V| = P_{ij}(o_2)\binom{t}{2} \qquad (13)$$

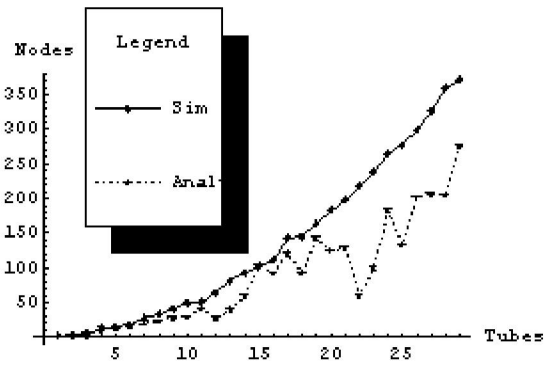

Fig. 11 Probabilistic analyses versus simulation results using actual tube lengths.

A maximum number of vertices are generated when the difference between the x, y values are small, that is a high concentration of tubes, when L is large, and when θ is $(+/-)\pi/4$ radians or $(+/-)3\pi/4$ radians. The concentration of tubes required for a connected network across the gate increases at these angles. The relation between L and θ to create a connected network for a given concentration of tubes in area wL_{sd} also needs to be determined. If tube lengths are held constant and each tube center is located farther apart, then tube angles must be reduced in order to achieve a connected graph, which will reduce the number of vertices. Thus, there is an optimal range of θ for a given area that meets the requirement for a connected graph, but that also maximizes (or minimizes) the number of vertices in the CNT network $G(V,E)$. The probability of a connected network comes from (8). The requirement for a network reaching from source to drain is the probability that tubes i and j are connected and that i and j cover the required distance. The expected distance covered that meets or exceeds the source to drain distance is shown in (14).

$$\sum_{i=1}^{n}\sum_{j=1, j\neq i}^{n} P_{ij}(o_2)\left(\left|x_i - x_j\right| + \left(\tfrac{L_i}{2}\cos\theta_i + \tfrac{L_j}{2}\cos\theta_j\right)\right) \geq L_{sd} \qquad (14)$$

Graph spectral analysis is used for analyzing the properties of the CNT graph. Fig. 15 shows the conductance of a CNT network that has random tube layouts with gate area 2 x 2 microns, tube density 1.5 tubes/sq micron, tube length of 2 microns and samples at tube angles of +/- {0,15,30,45,60,75, 90} degrees. The second lowest eigenvalue indicates graph connectivity (Fiedler value). These results show that there is very strong correlation between the second lowest eigenvalue and both the percolation threshold and the conductance (in units of Siemens which is the inverse of resistance). Note that at zero degree angles, single tubes spanned the source drain allowing for a relatively high conductance.

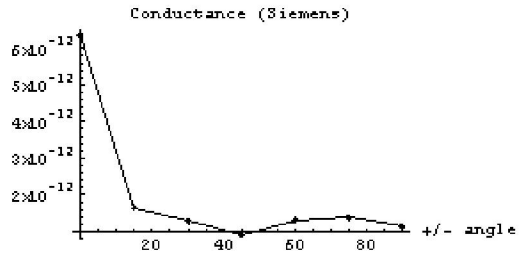

Fig. 12 Network resistances versus range of tube angles.

In Fig. 13, the second smallest eigenvalue of the graph Laplacian is plotted for each of the same tube layouts as in the previous figure. Note is the similar trend in this plot and the previous plot of conductance.

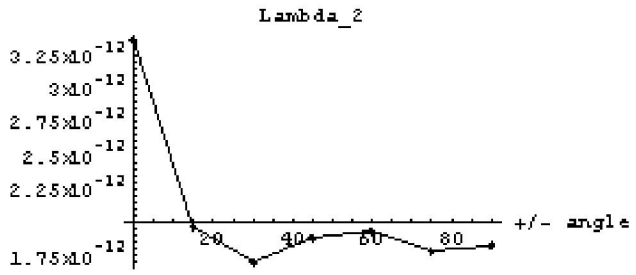

Fig. 13 The second smallest Eigenvalue of the Graph Laplacian versus the range of tube angles.

The probability of percolation is the probability that a given tube layout will have connectivity from source to drain. It is determined by using the same network parameters as in the previous figures, namely tube density, area, and length and analyzing many layouts with each set of tube angles. The results are shown in Fig. 14.

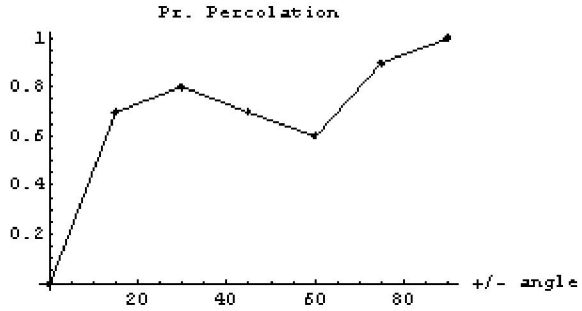

Fig. 14 The probability of achieving percolation as a function of ranges of tube angles. A larger range of tube angles (higher tube entropy) increases the probability of percolation.

The most important point of these results is that the second smallest eigenvalue of the graph Laplacian does indeed correlate strongly with both total conductance of the network and the probability of percolation as shown in Fig. 15.

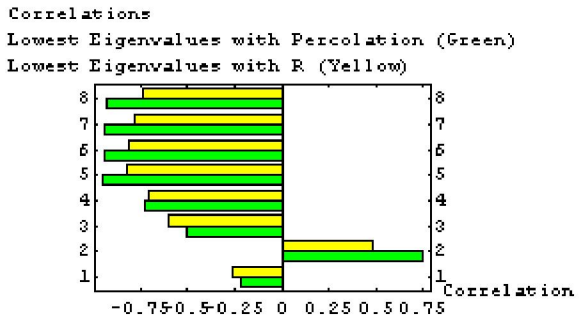

Fig. 15 The correlation of the lowest eight graph laplacian eigenvalues with both the probability of percolation and the network resistance.

III. Data Transmission in a CNT Network

Data transmission occurs via modulated current flow through the CNT network guided towards specific nano-destination addresses. The addresses identify spatially distinct areas of the CNT network. Since gate control is used to induce routes through the CNT network (discussed in detail next), nano-addresses are directly mapped to combinations of gates to be turned on that induce a path from a source to a destination. Fig. 16 shows a conceptual view of the CNT network infrastructure. Note that in addition to gate routing control, sensors are often constructed directly from nanotubes in such a manner as to change the resistance based upon the amount and specificity of the material being sensed [10]. Thus, the act of sensing may change the routing through the network.

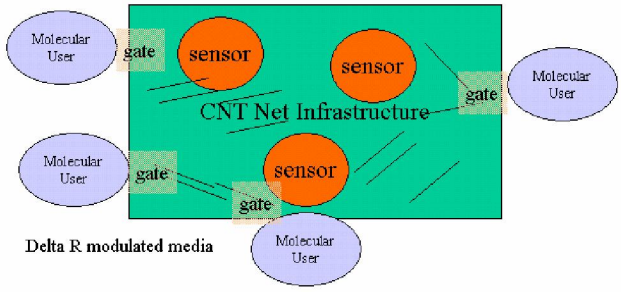

Fig. 16 The CNT network infrastructure is comprised of resistance-modulated media routing information among molecular-level addresses.

IV. Routing in a CNT Network

Given a CNT network, the mechanism used to route data through such a network must be considered. Consider a random CNT network with a matrix of gates as shown in Fig. 17. The gates are identified by number and when turned on, change the resistance of the semiconducting nanotubes within its area. Most nanotube sensing devices operate by changing tube resistance. A gate that is turned on, for any reason, may be used to route data through the network. Thus, the sensing elements, which sense by variation in resistance, may act simultaneously as routing elements. When a gate is turned on, the nanotubes within the gate area become conducting. Properly choosing gates to turn on also changes the current flow to the edges of the CNT network, effectively creating a controlled network, which may act as a communications network.

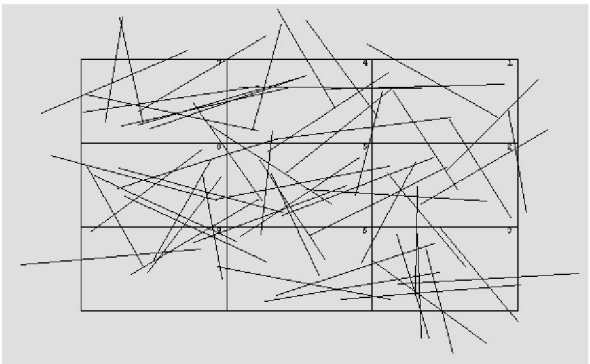

Fig. 17 Above is a matrix of gates superimposed on a random CNT network.

The potential for such routing capability is simulated using a specific CNT network shown in Fig. 18. The tubes shown in red are considered the outputs of this switch. Tube 52 is

considered the input. The hypothesis is that in this anisotropic media, tubes are randomly dispersed at all possible angles providing an approximately equal propagation of current in all directions. Activating gates appropriately serve to channel the flow into desired directions.

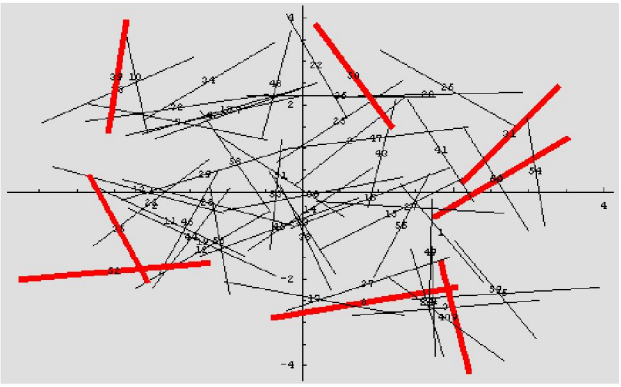

Fig. 18 Tubes used for I/O when the CNT network is used as a communication network are shown in red. The red tubes correspond to I/O contacts, one for each area surrounding the network (areas shown in previous figure).

Using a relatively small 3 x 3 gate matrix, consider all 9 choose 3 possible combinations of gates turned on and the impact on the predefined output tubes. In this simple demonstration, we are checking the impact of every possible gate state on the flow of information through the network. The ratio of the resistances from tube 52 to all output tubes when no gates are turned on R_{off}, to the resistance between same tube pair when combinations of the gates are turned on R_{on} for selected I/O tubes is plotted on bar charts as shown in Fig. 19. The gates turned on that generate the bar chart values are shown beneath each bar chart. The last number in the list below each bar graph is the resistance threshold distinguishing the output resistance ratio from the next highest ratio.

The effectiveness of the routing capability is measured by the difference between the resistance ratio at each output and the expected resistance ratio at all outputs (15); only the most effective gate combination is shown for each output.

$$\max_{ongates}\left[\left(R_{off}/R_{on}\right)_{target Output} - E_{outputs}\left[R_{off}/R_{on}\right]\right] \qquad (15)$$

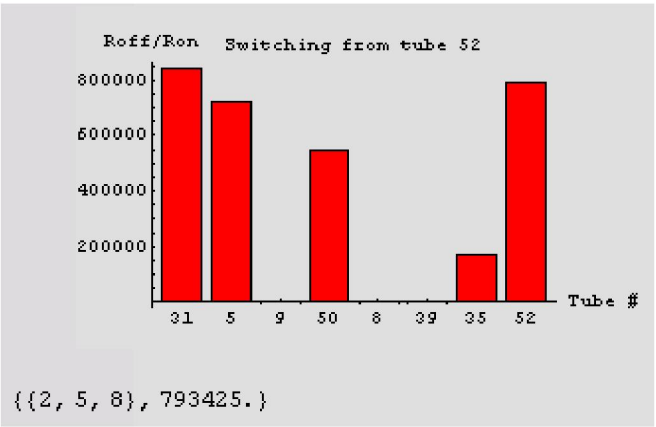

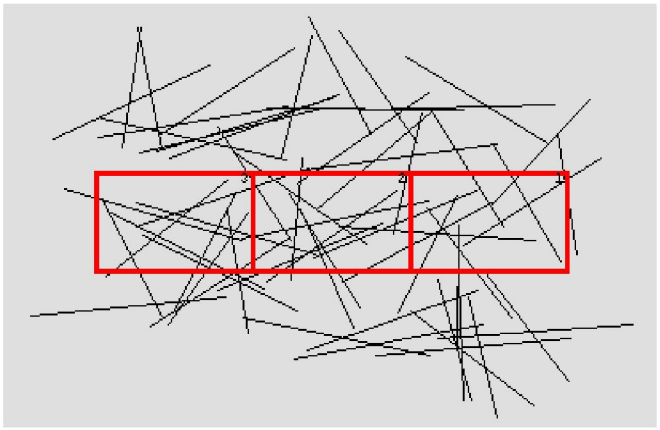

Resistance ratio and gate configuration for output tube 31.

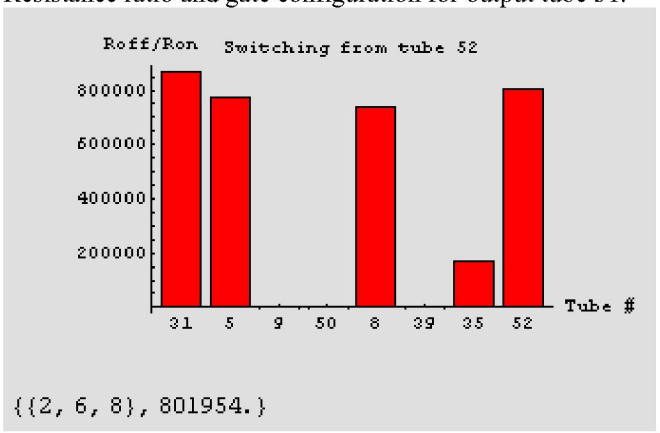

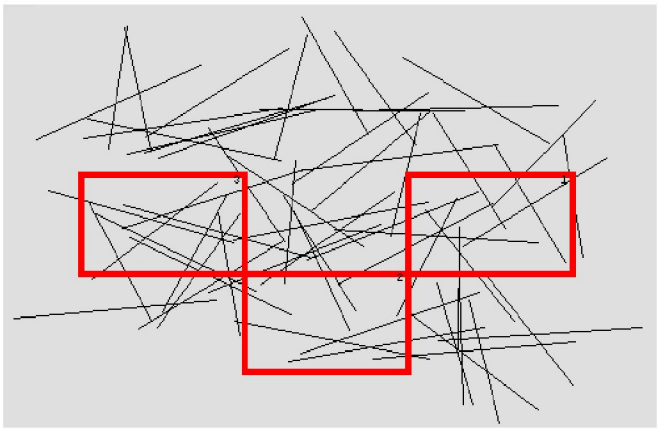

Resistance ratio and gate configuration for output tube 5.

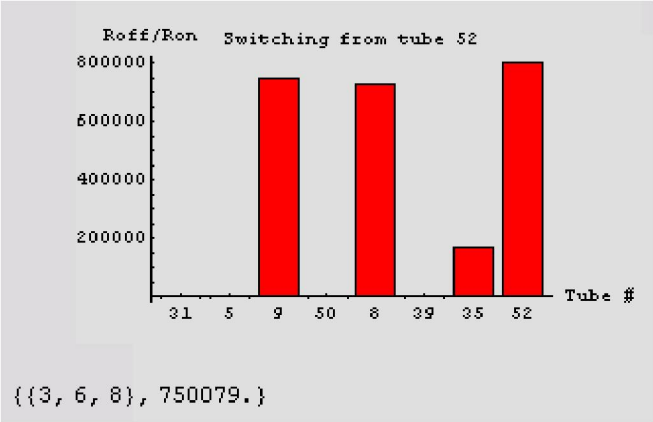

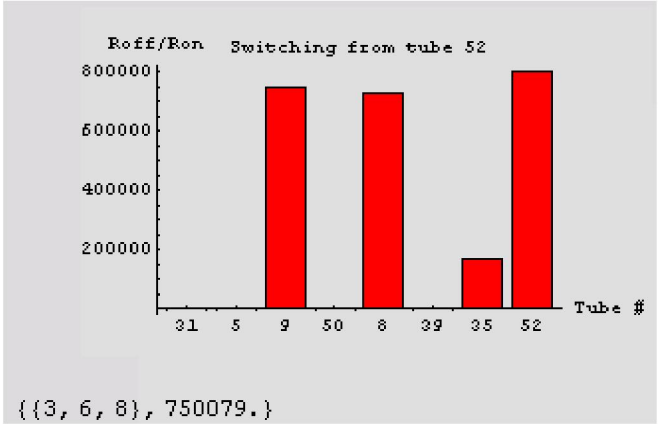

Resistance ratio and gate configuration for output tube 9.

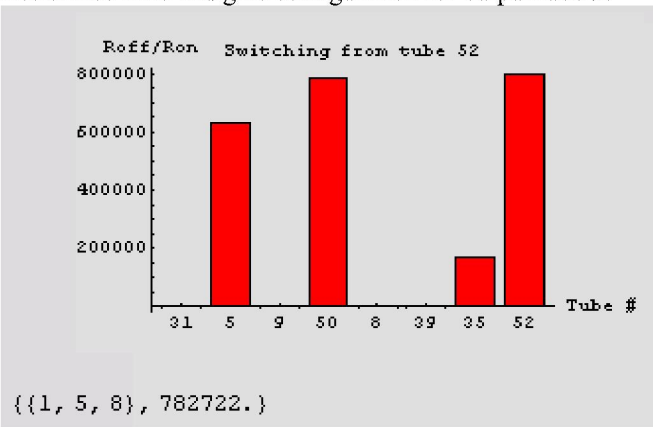

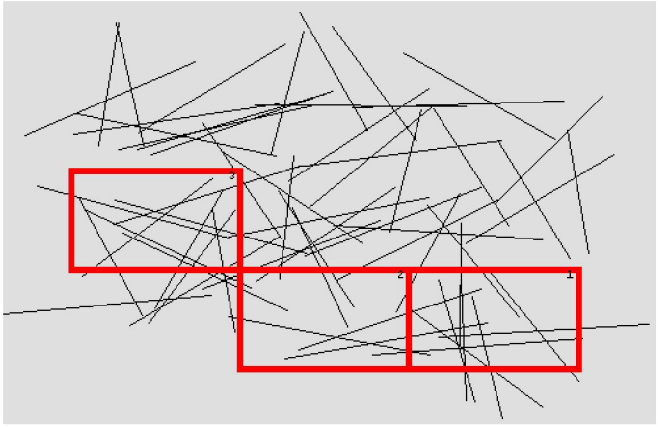

Resistance ratio and gate configuration for output tube 8.

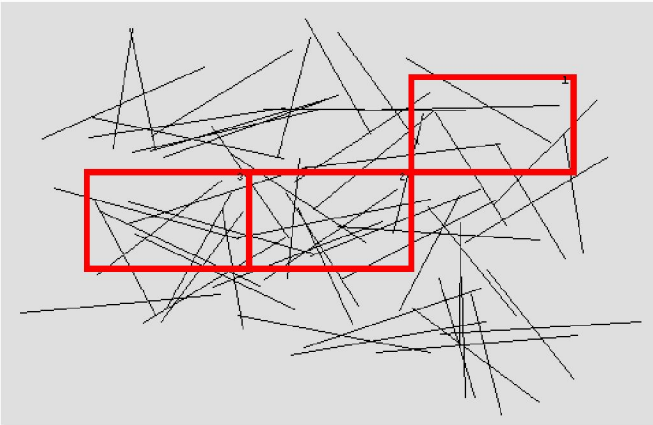

Resistance ratio and gate configuration for output tube 50.

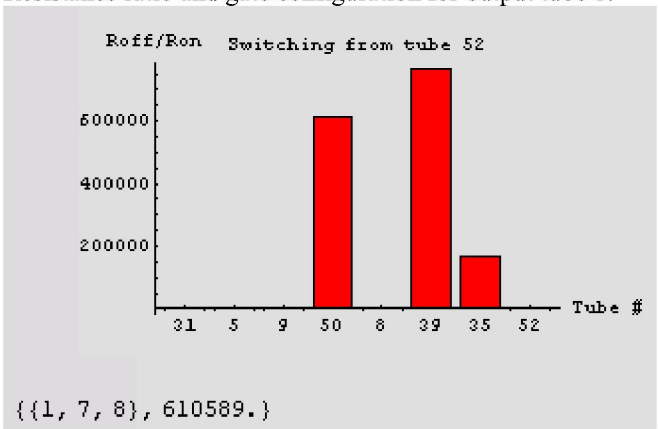

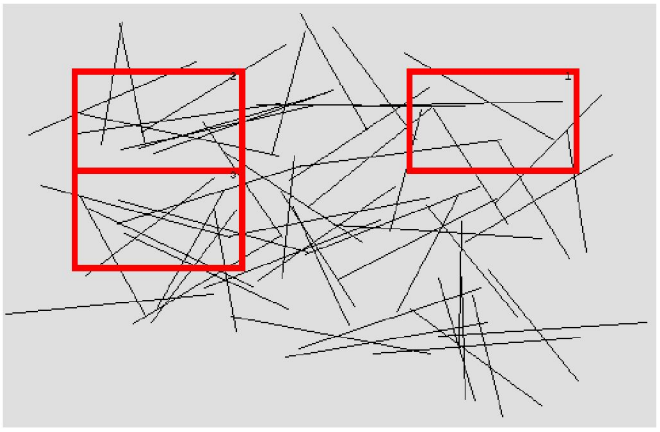

Resistance ratio and gate configuration for output tube 39.

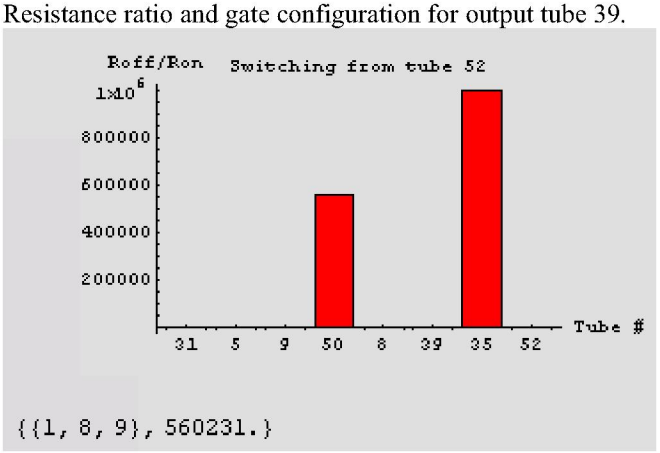

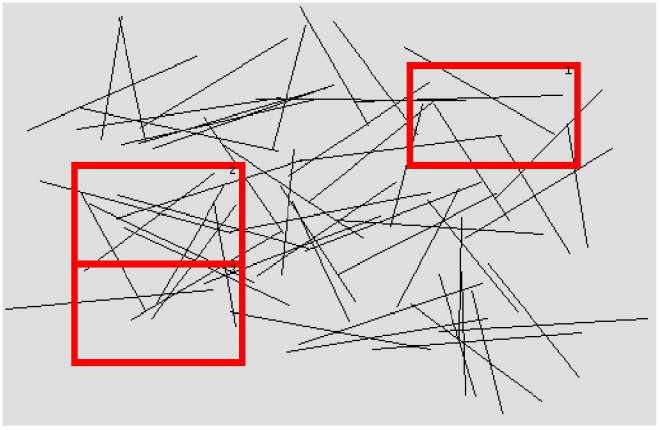

Resistance ratio and gate configuration for output tube 35.

Fig. 19 The ratio of resistance with no gates turned on to the resistance with the indicated gates turned on is shown in the bar graphs for selected I/O tubes.

V. Conclusion

Information flow through a CNT network may be controlled in spite of the random nature of tube alignment. The same technique used for sensing in CNT networks, namely, change in resistance of semiconducting material, may be used to effectively route information. The traditional networking protocol stack is inverted in this approach because, rather than the network layer being logically positioned above the physical and link layers, the CNT network and routing of information is an integral part of the physical layer. The potential benefits of better utilizing individual nanotubes within random carbon nanotube networks (CNT) to carry information is distinct from traditional, potentially less efficient and wasteful, approaches of using CNT networks to construct transistors which are then used to implement communication networks. In closing, the author would like to pose some theoretical questions with significant practical impact, namely, (1) whether one might achieve an information rate through the CNT network that approaches the maximum flow through the equivalent network graph, in other words, network coding at the level of individual nanotubes [7] and (2) whether given a network resistance, one could generate the underlying tube layout. That is, given a network resistance (as well as minimal information regarding tube characteristics), one can generate a set of feasible tube layouts with the given resistance. This may be approached via the inverse eigenvalue problem.

VI. Acknowledgement

I would like to thank Yun Li for his helpful and constructive comments and insight into the operational aspects of carbon nanotubes.

References

[1] Bush, S. F. and Smith, N., The Limits of Motion Prediction Support for Ad hoc Wireless Network Performance, The 2005 International Conference on Wireless Networks (ICWN-05) Monte Carlo Resort, Las Vegas, Nevada, USA, June 27-30, 2005.

[2] Bush, S.F. and Li, Yun. "Network Characteristics of Carbon Nanotubes: A Graph Eigenspectrum Approach and Tool Using Mathematica," GE Global Research, Technical Report, 2006GRC023, January 2006.

[3] Bush, Stephen F. and Li, Yun, "Network Characteristics of Carbon Nanotubes: The Impact of a Metallic Nanotube on a CNT Network," GRC Technical Report in press.

[4] Cai, H., Cao, X., Jiang, Y., He, P., Fang, Y. Carbon nanotube-enhanced electrochemical DNA biosensor for DNA hybridization Detection, Analytical and Bioanalytical Chemistry, Springer, 2003.

[5] Dasgupta, A., Hopcroft, J.E., McSherry, F. (2004) Spectral Analysis of Random Graphs with Skewed Degree Distributions, 45th Annual IEEE Symposium on Foundations of Computer Science, Rome, Italy, pp. 602-610.

[6] Gupta, P. and Kumar, P.R. "Capacity of wireless networks," Technical report, University of Illinois, Urbana-Champaign, 1999.

[7] Kramer, Gerhard and Savari, Serap A., "Edge-Cut Bounds On Network Coding Rates," Journal Of Network And Systems Management, Vol. 14, No. 1, March 2006, Special Issue On Management Of Active And Programmable Networks, Guest Editors: Stephen Bush And Shivkumar Kalyanaraman.

[8] Mihail, M., Papadimitriou, C.H., and Saberi, A. (2003) On Certain Connectivity Properties of the Internet Topology, 44th Annual IEEE Symposium on Foundations of Computer Science, Cambridge, MA.

[9] Wolf, E. L. Nanophysics and Nanotechnology. ISBN 3-527-40407-4, Wiley-VCH, 2004.

[10] Wolfram, S. The Mathematica Book, Fifth Edition, Wolfram Media, ISBN 1-57955-022-3, 2003.

STEPHEN F. BUSH (M'03-SM'03) is a researcher at GE Global Research. He continues to explore novel concepts in complexity and algorithmic information theory with a spectrum of applications ranging from network security and low energy wireless ad hoc sensor networking to DNA sequence analysis and bioinformatics.

Email: bushsf@research.ge.com
PH: (518) 387-6382
FX: (518) 387-4042
URL: http://research.ge.com/~bushsf

Sanjay Goel is an Assistant Professor in the School of Business at the University at Albany, SUNY. He is also the Director of Research at the New York State Center for Information Forensics and Assurance at the University. Before joining the University, he worked at the General Electric Global Research Center. Dr. Goel received is Ph.D. in Mechanical Engineering in 1999 from Rensselaer Polytechnic Institute. His current research interests include investigation of computer crimes including botnets and virus/worm propagation, security risk analysis and security policy creation. He also works in the development of autonomous computer security systems based on biological paradigms of immune systems, epidemiology, and genetics. His portfolio of research includes distributed service-based computing, network resilience, and active networks. He also uses machine-learning algorithms to develop self-learning adaptive optimization strategies for solving engineering optimization problems. In addition, he is working on developing algorithms for self-organization of nanosensors for remote sensing in harsh environments in collaboration with the College of Nanoscale Sciences and Engineering at the University at Albany.

Email: goel@albany.edu
PH: (518) 442-4925
FX: (518) 442-2568
URL: http://www.albany.edu/~goel/